



Design, synthesis and cruzain docking of 3-(4-substituted-aryl)-1,2,4-oxadiazole-*N*-acylhydrazones as anti-*Trypanosoma cruzi* agents

José Mauricio dos Santos Filho^{a,*}, Ana Cristina Lima Leite^b, Boaz Galdino de Oliveira^b,
Diogo Rodrigo Magalhães Moreira^b, Milena S. Lima^c, Milena Botelho Pereira Soares^{c,d},
Lucia Fernanda C. C. Leite^e

^a Departamento de Engenharia Química (DEQ), Centro de Tecnologia e Geociências, Universidade Federal de Pernambuco (UFPE), Rua Prof. Artur Sá S/N, Cidade Universitária, 50740-521 Recife, PE, Brazil

^b Departamento de Ciências Farmacêuticas (DCFAR), Centro de Ciências da Saúde, UFPE, Rua Prof. Artur Sá S/N, Cidade Universitária, 50740-520 Recife, PE, Brazil

^c Centro de Pesquisas Gonçalo Moniz, Fundação Oswaldo Cruz (FIOCRUZ), Rua Waldemar Falcão, 121, Candeal 40296-750, Salvador, BA, Brazil

^d Hospital São Rafael, Av. São Rafael, 2152, São Marcos 41253-190, Salvador, BA, Brazil

^e Universidade Católica de Pernambuco (UNICAP), Rua do Príncipe, 560, Boa Vista, 50050-900 Recife, PE, Brazil

ARTICLE INFO

Article history:

Received 12 May 2009

Revised 22 July 2009

Accepted 26 July 2009

Available online 6 August 2009

Keywords:

Trypanosoma cruzi

Oxadiazole

N-Acylhydrazone

Privileged structures

Molecular docking

Cruzain

ABSTRACT

Research in recent years has demonstrated that the *Trypanosoma cruzi* cysteine protease cruzain (TCC) is a valid chemotherapeutic target, since inhibitors of this protease affect the pathology appropriately. By exploring the *N*-acylhydrazones (NAH) as privileged structures usually present in antiparasitic agents, we investigated a library of 16 NAH bearing the 3-(4-substituted-aryl)-1,2,4-oxadiazole scaffold (NAH **3a–h**, **4a–h**). The in vitro bioactivity against epimastigote and trypomastigote forms of *T. cruzi* was evaluated, and some NAH under study exhibited antitrypanosomal activity at concentrations that are not toxic to mammalian cells. The series of compounds based on the 3-(4-substituted-aryl)-1,2,4-oxadiazole scaffold revealed the remarkable importance of each substituent at the phenyl's 4-position for the inhibitory activity. Non-nitrated compounds **3a** and **4e** were found to be as potent as the reference drug, Benznidazole. In addition, the molecular origin of the antitrypanosomal properties for these series was investigated using docking studies of the TCC structure.

© 2009 Elsevier Ltd. All rights reserved.

1. Introduction

Chagas' disease or American trypanosomiasis, caused by the protozoon, *Trypanosoma cruzi*, and transmitted to humans by infected blood-sucking reduviid bugs of the subfamily *Triatominae*, continues to afflict millions of people in Latin American countries. The treatment of Chagas' disease is heavily reliant on chemotherapy using Benznidazole (**Bdz**), the only World Health Organization-recommended drug. There are, however, major concerns regarding its high toxicity and low effectiveness during the chronic phase of infection.^{1,2} Therefore, there has been a considerable interest in trying to find novel approaches to drug design and biological targets, as new ways of combating the parasite.³

Molecular targets of the parasite, such as the cruzain,⁴ trypanothione reductase⁵ and *trans*-sialidase⁶ of *T. cruzi* have proved to be useful for the medicinal chemistry of new anti-*T. cruzi* drug candidates.⁷ The *T. cruzi* cruzain (TCC) is a member of the papain superfamily of cysteine proteases, with structure and functions similar to the human enzymes cathepsins B, L, K, S, F, and V.⁸ This cysteine

protease is capable of degrading components of the extracellular matrix and is involved in the replication and nutrition of the parasite.⁹ In view of these roles, TCC has emerged as a potential target for drug development in Chagas' disease treatment.¹⁰

The first compounds investigated as potential TCC inhibitors were peptides and peptidomimetics functionalized using vinyl sulfones, epoxyketones or diazomethylketones groups. However, except for the family of dipeptidyl vinyl sulfones, it has generally been observed that most peptide inhibitors show low selectivity against related proteases (serine protease chymotrypsin), with a subsequent toxicity against the mammalian counterparts.¹¹

In order to avoid this undesirable pharmacological profile, the replacement of a peptide backbone by a more rigid central scaffold has been considered and, in this scenario, *N*-acylhydrazones (NAH) have provided medicinal chemists with a solid strategy for the design of parasite cysteine protease inhibitors (CPs), including cruzain, falcipain-2, rhodesain and *Leishmania* cpB (Fig. 1). In these initial studies, a set of NAH libraries were investigated, exploring diverse molecular modifications such as bioisosterism, molecular simplification and the development of congener series.^{12–15} Moreover, the use of NAH subunit has enabled the discovery of a number of lead compounds with potent and selective activity

* Corresponding author. Tel.: +55 81 21267288; fax: +55 81 21267278.

E-mail address: mauricio_santosfilho@yahoo.com.br (J.M. dos Santos Filho).

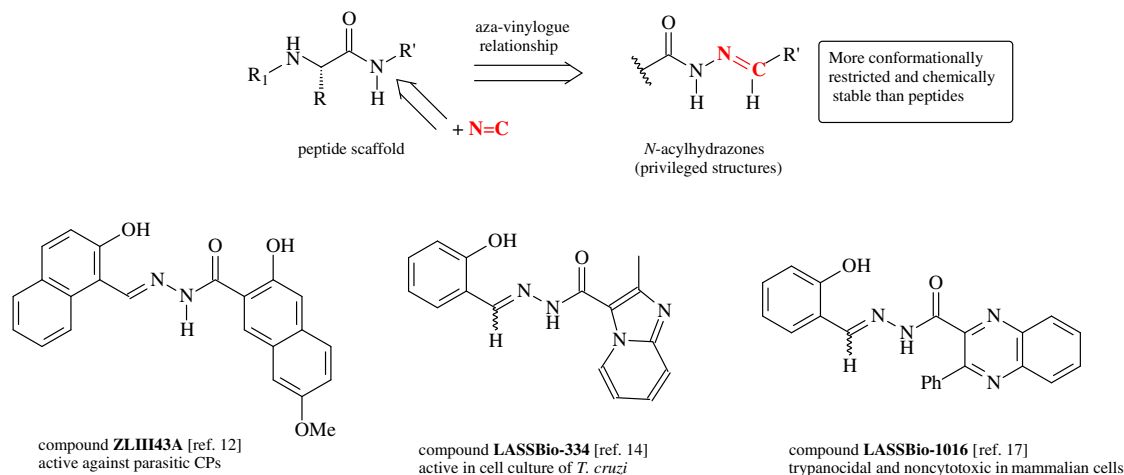


Figure 1. Design concepts for the NAH subunit as privileged structures.¹⁹ Structures of NAH derivatives described as inhibitors of parasitic CPs are listed above.

against the replication of *T. cruzi*.^{16,17} For example, the adequate combination of the NAH subunit attached to a quinoxaline ring resulted the discovery of two new antitrypanosomal agents with IC₅₀ values of 15.9–20 μM against epimastigotes of *T. cruzi* (Tulahuen 2 strain) at concentrations that do not overtly affect J774 mouse macrophages, as exemplified by LASSBio-1019 (Fig. 1). In the course of this work, in silico studies of molecular docking of these quinoxaline–NAH were conducted to establish substantial hydrogen bond interactions with the TCC structure, which possibly acted by way of targeting the TCC enzyme.¹⁶

From the point of view of medicinal chemistry, NAH are endowed with the interesting capacity of being able to interact with diverse bioreceptors, owing to their ability to establish H-bonding sites and the theoretical feasibility of adopting a unique conformational orientation.¹⁸ This profile suggested that the NAH subunit would be of crucial importance in the process of molecular recognition by the target. Another structural feature of the NAH moiety is its non-peptidic and achiral nature, which, in addition to its being synthetically treatable, thereby makes its suitable for performing structure–activity relationships (SARs). It stands to reason that the NAH have assumed the position of authentic privileged structure for the structural design of new drug candidates, as recently reviewed by Barreiro and co-workers.¹⁹

In this study, we report the synthesis of two new series of 3-(4-substituted-aryl)-1,2,4-oxadiazole-*N*-acylhydrazones and their in vitro activity against epimastigote and trypomastigote forms of *T. cruzi*, as well as their interaction with the TCC structure, as determined by molecular docking studies. In our design, the oxadiazole heterocycle was selected as a trypanocide scaffold, for reason of its previously observed antiparasitic properties,²⁰ and because it is recognized as an amide bioisoster, in addition to being chemically more stable than peptide bonds²¹

2. Chemistry

2.1. Synthesis

The substituted 3-(4-substituted-aryl)-1,2,4-oxadiazolyl-*N*-acylhydrazones **3a–h** and **4a–h** (Scheme 1) were prepared from arylamidoximes. After the cyclocondensation reaction between arylamidoximes and methyloxalyl chloride under reflux in dry THF, the intermediates bearing an 1,2,4-oxadiazole ring (**1a–h**) were obtained and then converted into 1,2,4-oxadiazolylcarbohy-

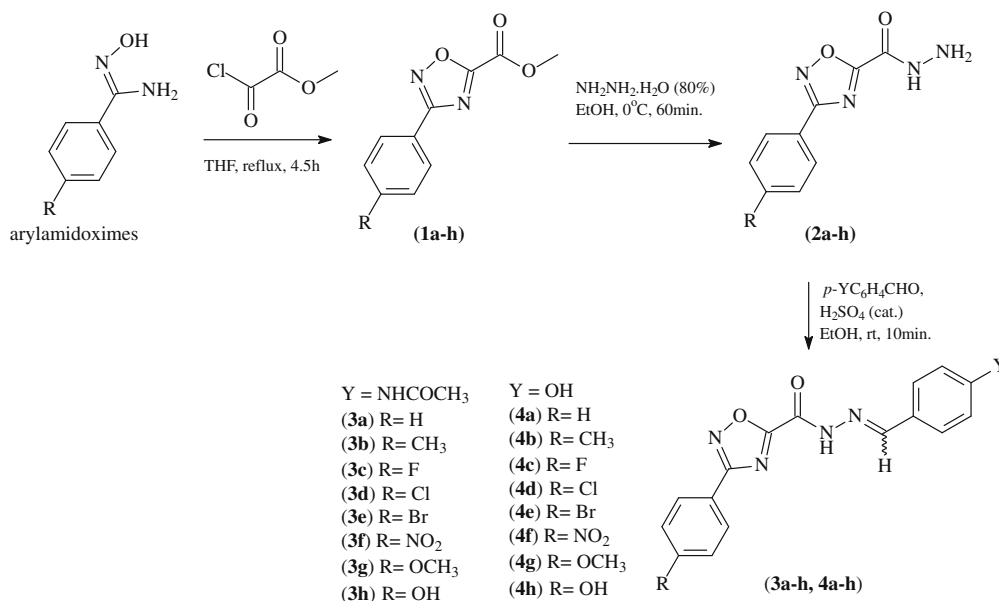
razides (**2a–h**) by reaction with hydrazine hydrate in ethanol at 0 °C for the duration of 60 min.²²

Usually, the condensation reaction between hydrazides and appropriate 4-substituted phenylaldehydes is achieved by refluxing the reactants under acid catalysis in protic solvent. However, a mixture of *Z/E*-isomers is often reported, mainly for reaction procedures that are only possible at high temperatures or for prolonged reaction periods. In a prior study involving the synthesis of *N*-acylhydrazone derivatives, a method employing free-catalyst conditions under reflux developed by our group yielded the *E*-isomers as major products, although with long reaction times (4 h).²³ Theoretical calculations for the configurational and conformational energies of these *Z/E*-isomers showed that a planar and more stable conformation for the *E*-isomer is achieved, this being the thermodynamically preferable product.

Recently, a report described that the NAH derivatives can be satisfactorily synthesized under acid catalysis for 30 min at rt.²⁴ This mild and rapid procedure was also observed in our laboratory during the synthesis of NAH derivatives. Interestingly, only a very short reaction time (10 min) was required to furnish the desired products, **3a–h** and **4a–h**, in very good to excellent yields with no detected by-products. Some physical and chemical properties of these NAH are summarized in Table 1.

2.2. Molecular modeling

Analysis of the structures and conformation of compounds **3a–h** and **4a–h** was carried out using the AM1 method,²⁵ available as part of the BIOMEDCACHE suite of programs,²⁶ using internal default settings as convergence criteria. Each of the most stable conformers of the *E*-isomers was subsequently selected for the docking analysis. The docking analysis was carried out on the TCC binding site (PDB code: 1U9Q),^{27,28} where the enzyme's residues are in close proximity to the inhibitor named as '186', a fluoromethyl ketone dipeptide that was co-crystallized in complex with the cruzain. This crystal structure is the monomeric catalytic domains termed X and the active site was narrowed down to all atoms within a sphere of radius 5.0 Å, as determined by the co-crystallized ligand '186'. The GOLD 4.0 program and HERMES²⁹ interface software were used for docking calculations, and all solvent molecules and the co-crystallized inhibitor were removed from the structure. The theoretical binding profile proposed for **3a–h** and **4a–h** ligands with TCC was determined as the highest (most positive) scored of 10 possible solutions for each ligand, ranked according to their fitness scores calculated using the GOLD docking function. We decided



Scheme 1. Synthesis of NAH **3a-h** and **4a-h**.

Table 1
Physical and chemical properties and parameter of bioavailability for the NAH **3a-h** and **4a-h**

Compd	R	Molecular formula ^a	Yield ^b (%)	Ratio ^c (<i>E</i> : <i>Z</i>)	C log <i>P</i> ^d
3a	H	C ₁₈ H ₁₅ N ₅ O ₃	90	100:0	2.19
3b	CH ₃	C ₁₉ H ₁₇ N ₅ O ₃	95	100:0	2.79
3c	F	C ₁₈ H ₁₄ N ₅ O ₃ F	93	100:0	2.45
3d	Cl	C ₁₈ H ₁₄ N ₅ O ₃ Cl	98	100:0	2.91
3e	Br	C ₁₈ H ₁₄ N ₅ O ₃ Br	83	100:0	3.03
3f	NO ₂	C ₁₈ H ₁₄ N ₆ O ₅	90	100:0	2.28
3g	OCH ₃	C ₁₉ H ₁₇ N ₅ O ₄	89	100:0	2.30
3h	OH	C ₁₈ H ₁₅ N ₅ O ₄	91	100:0	1.76
4a	H	C ₁₆ H ₁₂ N ₄ O ₃	98	88.9:11.1	2.50
4b	CH ₃	C ₁₇ H ₁₄ N ₄ O ₃	95	91.7:8.3	2.89
4c	F	C ₁₆ H ₁₁ N ₄ O ₃ F	85	90.9:9.1	2.63
4d	Cl	C ₁₆ H ₁₁ N ₄ O ₃ Cl	95	90.9:9.1	3.09
4e	Br	C ₁₆ H ₁₁ N ₄ O ₃ Br	88	91.7:8.3	3.20
4f	NO ₂	C ₁₆ H ₁₁ N ₅ O ₅	85	91.7:8.3	2.47
4g	OCH ₃	C ₁₇ H ₁₄ N ₄ O ₄	90	88.9:11.1	2.49
4h	OH	C ₁₆ H ₁₂ N ₄ O ₄	85	91.7:8.3	2.03

^a Determined by HRMS.

^b Calculated from purified products.

^c Determined by the relative integration of the NHCOCH₃ (**3a-h**) or NH (**4a-h**) signals (¹H NMR, 200 MHz) for each isomer.

^d Using the ALOGPS 2.1 database.³³

to evaluate the binding patterns of compounds **3a-h** and **4a-h** at the TCC active site in theoretical docking terms, and compare these results with ligand '186' and also with the trypanocidal reference drug, **Bdz**.

3. Pharmacology

3.1. Assessment of cytotoxicity and antitrypanosomal properties

The *in vitro* cytotoxicity of all compounds was evaluated in cultures of mouse splenocytes, and expressed as the highest non-cytotoxic concentration for spleen cells. The compounds were then tested *in vitro* against epimastigote (proliferative) and trypomastigote (bloodstream) forms of *T. cruzi* (Y strain). Anti-*T. cruzi* properties were expressed in terms of the IC₅₀ (μM) values, calculated

after 11 days for epimastigotes and 24 h for trypomastigotes of treatment with each drug. Benznidazole (**Bdz**) and Gencian Violet (**GV**) were used as reference trypanocidal drugs. The SARs were qualitatively discussed on the basis of the chemical substitutions performing on the aromatic ring.

3.2. Toxicity in mice

The two most potent NAH derivatives were submitted to an assay for general toxicity in mice treated intraperitoneally with compounds **3a** and **4e** at a single dose of 100 mg/kg. Animals were monitored for signs of general toxicity, including behavior and feeding, until 72 h after treatment.

4. Discussion

The analysis of the ¹H NMR spectra of the crude product revealed that most **3a-h** compounds essentially adopted the *E*-configuration in solution and only in some cases were traces of *Z*-isomers observed (Table 1). The isomeric ratio of NAH derivatives was appropriately established by specific signals in the ¹H NMR spectra and confirmed on the basis of data reported in the literature.^{23,24} For instance, the NH protons of compounds **3a-h** allow this attribution, albeit with a remarkable tendency to undergo rapid exchange with the solvent. Fortunately, the NHCOCH₃ proton also generates specific signals for each isomer and furnishes a better evaluation set because neither superimposition with aromatic protons nor considerable exchange occurs. On analysis of the splitting of the NH of acetamide, the signal at higher chemical shift values was attributed to the *E*-isomers, while, in the case of the *Z*-isomers the NH proton has a lower deshielding effect. Likewise, signals associated with the aromatic ring could be of value in determining this diastereomeric relationship, though in some cases superimposition of signals led to quantitative limitations.

The *E/Z*-ratio for the **4a-h** series behaved differently, since the *Z*-isomers constituted 9–11% of the diastereomeric mixture, despite the fact that no special effort had been made to isolate them. Tautomerism may be involved during the formation of *Z*-isomer, given that it is theoretically feasible that the hydroxyl group may

play a part in tautomeric equilibrium in solution via a proton transfer. This kind of tautomerism is consistent with the lability and free rotation required to form the Z-isomer from the E-isomer, although additional experimental data are not available at present. The suggested tautomeric conversion is depicted in Scheme 2. In addition to the pair of signals associated with the NH of the acyl-hydrazone group and to the split aromatic protons characterizing the E/Z-isomers, the series of compounds, **4a–h**, exhibited two different signals attributed to the hydroxyl group at around $\delta = 10.08$ ppm (E-isomer) and at $\delta = 9.99$ ppm (Z-isomer), reinforcing the qualitative analysis.

Once their structure had been elucidated, all compounds were tested as antitrypanosomal agents and the results of this are shown in Table 2. The **3a–h** series shares an acetamide group, while the molecules of the **4a–h** series bear a hydroxyl group. Such groups were selected because of the chemical reactivity of hydroxyl and the neutral nature of the acetamide. In medicinal chemistry, the acetamide is considered to be the simplest model for a peptide fragment. Besides, both chemical groups are endowed with the capacity to form intermolecular hydrogen bonds with biological targets. It was observed that such groups generated two distinct sets of antitrypanosomal agents, and the SARs will first be discussed separately for each series.

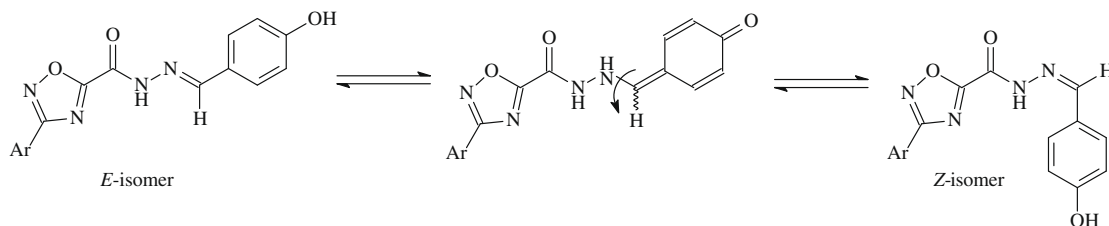
Analysis of the NAH belonging to the **3a–h** series showed that the non-substituted derivative **3a** was very active against epimastigote and trypomastigote forms of *T. cruzi* at non-cytotoxic concentrations. On comparing the inhibitory activity of **3a** and the analogue methyl substituted **3b**, the latter proved to be more active and to have a potency similar to that of **Bdz**, although of higher cytotoxicity among the **3a–h** series. By contrast, on replacement of

methyl by other substituents (compounds **3c–3h**), these inhibitory properties were lost.

For the **4a–h** series of NAH, it was initially observed that, although of moderate potency against the trypomastigote, the non-substituted derivative **4a** was inactive against the epimastigote form. The replacement of an hydrogen (**4a**) by methyl (**4b**) or methoxy (**4g**) at the *para*-position improved potency against both forms of the parasite, but a concomitant loss of selectivity was observed in **4b**. The potency of methyl (**4b**) and fluorine (**4c**) derivatives was also compared, since methyl and fluorine are of similar size. The fluorine was twice as potent as the methyl derivative against epimastigote, although the two were equipotent against the trypomastigote form.

Analysis of the NAH derivatives bearing halogen substituents gave rise to the observation of interesting SAR. Compared with the non-halogenated parent, **4a**, each one of the *para*-halogenated analogues exhibited an increase in the antitrypanosomal activity, the order of potency being: **4c** (F) > **4e** (Br) = **4d** (Cl). In fact, these differences in potency are consistent with the molecular modification performed, because the influence of halogen substituents on biomolecular interactions does not occur because of steric differences alone, but also as a result of modification of thermodynamic parameters.³² Apart from the bromine, **4e**, which was capable of inhibiting the parasite at non-cytotoxic concentrations against mammalian counterparts, the chlorine, **4d**, and fluorine, **4c**, derivatives were cytotoxic for the mammalian cells.

The nitro derivative (**4f**) was as potent as the halogenated derivatives, but it proved cytotoxic in mammals. The hydroxyl derivative (**4h**) exhibited the weakest antitrypanosomal activity of the entire series. In fact, the **4h** also exhibited the lowest *c log P* value



Scheme 2. Proposal of the tautomeric forms in solution, resulting the formation of Z-isomers.

Table 2

In vitro anti-*Trypanosoma cruzi* activity of NAH derivatives against Y strain

Compd.	R	Trypomastigotes IC ₅₀ in μM^a	Epimastigotes IC ₅₀ in μM^a	Cytotoxicity ^b ($\mu\text{g/mL}$)
3a	H	3.6	14.2	33 (95)
3b	CH ₃	3.9	9.8	11 (30)
3c	F	Nd.	>150	33
3d	Cl	Nd.	>150	100
3e	Br	Nd.	>150	33
3f	NO ₂	Nd.	>150	33
3g	OCH ₃	Nd.	>150	100
3h	OH	Nd.	>150	33
4a	H	35.7	78.3	3.3
4b	CH ₃	17.9	47.8	<1.1
4c	F	16.7	21.0	<1.1
4d	Cl	21.2	21.6	<1.1
4e	Br	20.5	19.6	33 (97)
4f	NO ₂	21.3	25.2	<1.1
4g	OCH ₃	32.5	13.8	33 (85)
4h	OH	100.3	126.6	100
Bdz ^c	—	5.0	6.6	100
GV ^c	—	2.1	—	<1.0

^a Calculated from seven concentrations using data obtained from at least three independent experiments (SD less than 10% in all cases). Nd., not determined, due to the lack of activity against epimastigotes.

^b Expressed as the highest concentration tested non-cytotoxic for mouse splenocytes. Values in μM are shown in parentheses.

^c **Bdz** is Benzimidazole and **GV** is Gencian Violet.

of the **4a–h** series (Table 1). One plausible explanation for this weak activity is the lipophilic effect, because low lipophilicity is often associated with problems regarding the permeability of the cell membrane.

In the light of these results, the structures of NAH **3a–h** and **4a–h** (*E*-isomers) were subjected to docking analysis of the TCC structure, in an effort to gain information on the molecular origin of the antitrypanosomal properties of these NHA derivatives. The GOLD program was used to identify favourable conformations and possible interaction regions at the active site of the enzyme. All the top-ranked conformations of **3a–h**, **4a–h** and **Bdz** were orientated in such a way as to insert themselves into the same pocket of the TCC structure, and their docked locations on the active site were very close to that occupied by the co-crystallized ligand '186'. Figure 2 shows a superimposition of these docking solutions alongside the docking of the ligand '186' that was co-crystallized with TCC.

In the light of this interesting finding, we decided to compare *in vitro* and *in silico* results in order to gain an understanding of the SARs of this family of NAH. This comparison appears to be relevant, given that the **3a–h** and **4a–h** NAH represent two congener series that share structural similarities and whose *in vitro* data for IC_{50} represent a quantitative parameter. Given this, the GOLD score was plotted against the pIC_{50} data (determined from IC_{50} values against trypanomastigotes). The results are shown in Table 3. In addition, for a better illustration of this comparison, some of the results in Table 3 were converted into Figure 3, although this illustration does not constitute a statistical correlation, but a comparison of *in vitro* and *in silico* results.

Analysis of this comparison suggests that, with the exception of a few outliers, the NAH derivatives with more stable GOLD scores on TCC were also the more potent *in vitro* antitrypanosomal agents. For example, Figure 3 shows that the **4e** and **4f** NAH, which are the most active of the **4a–h** series, also present the most positive scores, or conversely, possess higher (theoretical) affinity for the TCC structure.

In an attempt to explain the differences between the docking scores, an analysis of the polar interactions (hydrogen bonds) for the docked ligands on the active site of TCC structure are summarized in Table 4, along with the distances between the donor and acceptor atoms involved in this interaction by way of ligand–enzyme complexation. Additionally, details were provided of the docking positions for a number of NAH derivatives, along with the position of the crystallographic ligand '186' (Figs. 4–6). Docking positions were captured using the PYMOL v 0.99X program.^{30,31}

Table 3
Docking results for compounds **3a–h** and **4a–h**

Compd	R	Docking score ^a	Trypomastigotes	
			IC_{50} ^b (μ M)	pIC_{50} ^c
3a	H	45.08	3.6	5.44
3b	CH ₃	46.62	3.9	5.41
3c	F	44.41	Nd	—
3d	Cl	46.17	Nd	—
3e	Br	46.68	Nd	—
3f	NO ₂	45.22	Nd	—
3g	OCH ₃	45.95	Nd	—
3h	OH	43.45	Nd	—
4a	H	42.92	35.7	4.45
4b	CH ₃	44.30	17.9	4.75
4c	F	42.09	16.7	4.78
4d	Cl	44.10	21.2	4.67
4e	Br	46.32	20.5	4.69
4f	NO ₂	45.91	21.3	4.67
4g	OCH ₃	45.18	32.5	4.49
4h	OH	43.82	100.3	4.00
Bdz	—	43.83	5.0	5.30

^a The GOLD docking scores are dimensionless.

^b See corresponding footnotes in Table 2.

^c $pIC_{50} = 6 - (\log IC_{50})$ of Y strain trypanomastigotes, when IC_{50} values are given in μ M.

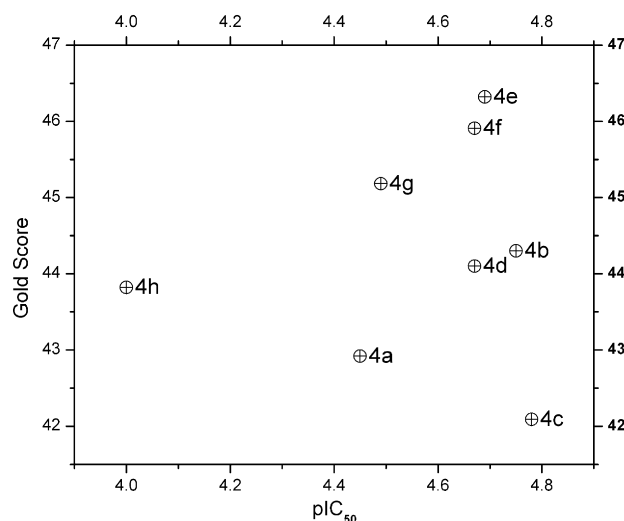


Figure 3. Comparison between the GOLD docking score and the pIC_{50} values (trypanomastigote, Y strain) for the series **4a–h**.

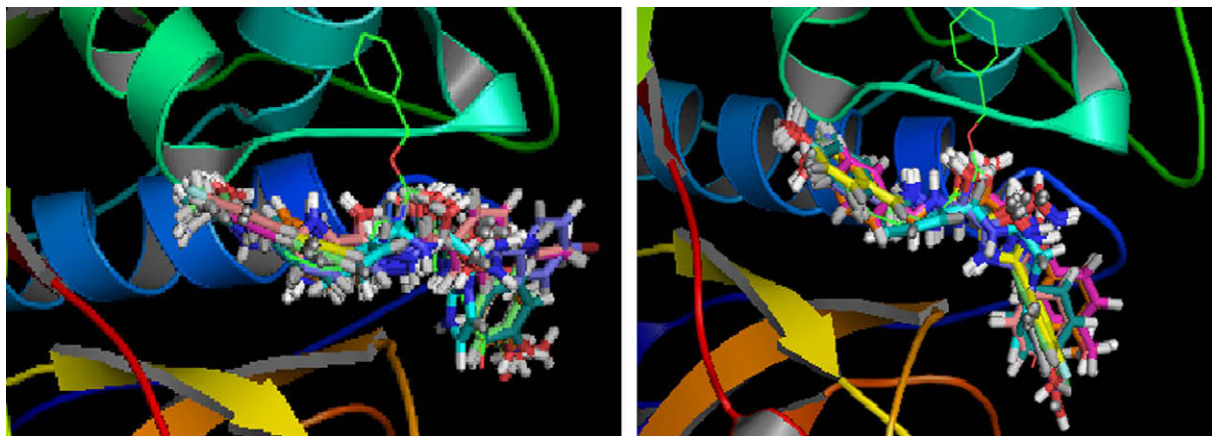
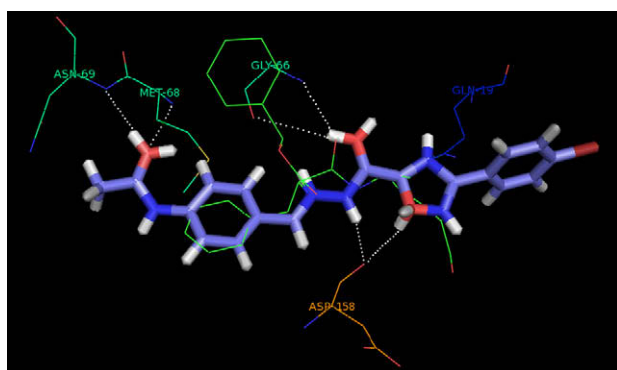
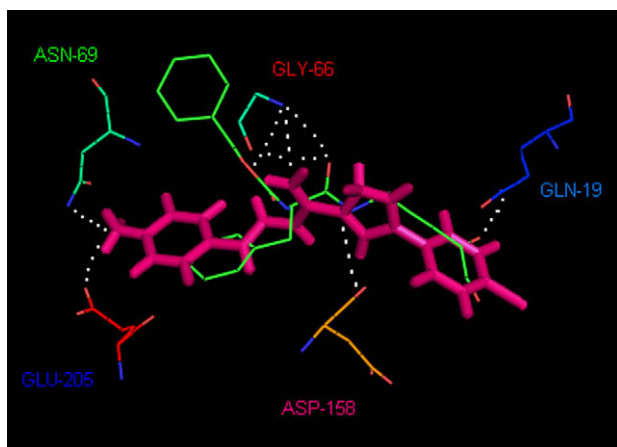


Figure 2. Superimposition of the highest ranked solution of *N*-acylhydrazones (stick model) in the binding site of TCC (ribbons model), as calculated by GOLD v. 4.0. Left: **3a–h** and **Bdz**; right: **4a–h** and **Bdz**, alongside the co-crystallized ligand '186' (wireframe model).

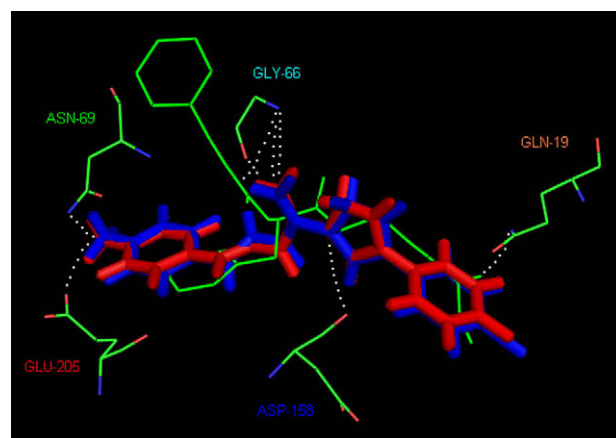
Table 4

Summary of the hydrophilic (H-phil) intermolecular interactions to the NAH in comparison with the co-crystallized ligand '186'

Ligands	Cruzain residues and distance of bonds ^a						
	Gln19	Glu205	Gly66	Asp158	Asn69	Cys25	Met68
'186'	2.84	—	3.05	3.12	—	—	—
Bdz	2.50–3.47	—	—	—	—	2.58–3.37	—
3^a	3.42	—	—	—	—	—	—
3b	—	—	—	1.76	3.44	—	2.99
3c	—	—	—	—	—	—	—
3d	—	—	—	2.48	—	—	2.97
3e	—	—	—	1.91	2.56	—	2.61
3f	—	—	—	2.86	2.50	—	2.73
3g	—	—	—	2.88	3.48	—	3.11
3h	—	—	—	2.93	3.42	—	2.78
4^a	—	2.80	2.91	—	—	—	—
4b	—	—	2.70	—	—	—	—
4c	—	1.66	3.08	—	2.95	—	—
4d	—	2.72	3.23	—	—	—	—
4e	—	1.83	3.29	—	3.56	—	—
4f	—	1.73	3.39	—	—	—	—
4g	—	—	2.81	—	—	—	—
4h	—	1.83	2.86	—	3.36	—	—

^a All values are given in angstroms.**Figure 4.** Docking pose of compound **3e** (stick model) alongside the co-crystallized ligand '186' (wireframe model) in the TCC binding pocket. White line represents the hydrogen bonding. Only the key residues are shown for clarity.**Figure 5.** Docked pose of compound **4e** (stick model) alongside the co-crystallized ligand '186' (wireframe model) in the TCC binding pocket.

The '186' inhibitor establishes hydrogen bonds with the key residues, Gln19, Gly66 and Asp158, with respective measurements of 2.84, 3.05 and 3.12 Å. Modeling indicated that the *N*-acylhydrazone subunit is accommodated on hydrophilic pocket of the active site

**Figure 6.** Docked pose of compounds **4g** (red) and **4h** (blue) alongside the co-crystallized ligand '186' (green, wireframe model) in the TCC binding pocket.

of the TCC, while that of the phenyl adjacent to the 1,2,4-oxadiazole ring is accommodated on a small hydrophobic pocket, located close to the Gln19 residue. It is worth pointing out that the molecules of the **4a–h** series establish a hydrogen bond (H-bond) with the Asp158 by way of the carbonyl group of the *N*-acylhydrazone subunit. On the other hand, interactions with the Asp158 residue for the **3a–h** series predominantly involve the nitrogen atom of the *N*-acylhydrazone subunit. Particularly noticeable are the interactions of the acetamide group (**3a–h** series) with the Met68 residue, while the hydroxyl group (**4a–h** series) is generally found to interact with the Glu205 residue. Furthermore, the pocket that the **4a–h** series occupies is hydrophobic in the vicinity of Gly66 and bounded by an electronegative region marked by Asp158 and Glu205. This provides one initial explanation for the difference in antitrypanosomal activity observed within the NAH series.

With regard to the SAR within **3e** and **4e**, the docking analyses provided a number of explanations. The **3e** derivative, which possesses a bromo substituent, was the NAH of those tested which presented the most stable GOLD score, but was inactive against the parasite. By contrast, another bromo analogue (**4e**) also presented a stable GOLD score, but in this case, it was much more potent in inhibiting the cell culture of parasites than **3e**. In fact, analysis of the TCC residues predicted by docking studies reveals

that these two compounds have slight differences in terms of docking interactions with the enzyme. Figure 4 shows the NAH derivative **3e** establishing H-bonds with the Asp158, Asn69 and Met68 residues, with distances of 1.91, 2.56 and 2.34 Å respectively, while Figure 5 shows that the NAH derivative, **4e**, forms H-bonds with Glu205, Gly66, and Asn69 of 1.83, 3.29, and 3.56 Å in length, respectively. Likewise, Figure 4 demonstrates that Asp158 is involved in the bidentate H-bond with the oxygen atom on the 1,2,4-oxadiazole ring and with the nitrogen (NH) in the amide group for derivative **3e**. This kind of interaction with the Asp158 residue is a singular observation and was not seen in other NAH derivatives in the course of this study. Therefore, despite the excellent GOLD score value, this specific interaction predicted for derivative **3e** apparently did not contribute to efficient interaction with the target.

Examination of the TCC complex with the **4g** and **4h** NAH showed that neither the hydroxyl (**4h**) nor the methoxy (**4g**) group establishes an H-bond with the enzyme (Figure 6), although **4g** results in a more stable complex (GOLD score) with the TCC than **4h**. In these cases, it is reasonable to suggest that the methoxy group gives rise to steric change, causing a favourable reorientation of the TCC pocket, which partly explains why **4g** is more potent than compound **4h**.

The final consideration regarding the in silico studies concerns the manner of inhibition of the TCC enzyme, that is, by covalent or non-covalent binding. Analysis of the general structures of the NAH reveals, from a theoretical point of view, that this subunit possesses sufficient reactivity to establish covalent interactions with protease, mainly when considering the resonance structures or tautomers, as previously highlighted.¹⁴ Finally, given the demonstrated potency of compounds **3a** and **4e**, it was decided to perform an acute toxicity assay in mice, using a single administration (ip) of 100 mg/kg. This experiment showed that the tested compounds (**3a** and **4e**) are non-lethal in mice, although the mice presented few behavioral signs after administration, and suggests that these are suitable for further in vivo studies of *T. cruzi* infection.

5. Conclusion

In conclusion, initial investigation of the medicinal chemistry of anti-*T. cruzi* agents resulted in the establishment of a set of SARs and the identification of new bioactive compounds. Among these, NAH **3a** and **4e** are especially worthy of note, as they proved to be potent antitrypanosomal agents and of low toxicity both in vitro and in vivo, assuming the position of lead-compounds. Notable chemical features of these two lead-compounds are their non-nitrated, non-peptidic and achiral natures, since such properties are considered as important criteria for the development of antitrypanosomal drug candidates.⁷ The docking patterns of the NAH series were similar to those of the '186' co-crystallized inhibitor, and display polar interactions with key residues of the active TCC site, such as Gly66, Asp158 and Asn69. The understanding of the manner of docking of our *N*-acylhydrazones on TCC was also consistent with the SARs observed, thereby providing a useful platform for a future structure-guided design of analogues with optimized potency.

6. Experimental protocols

6.1. Chemistry

Melting points were determined on a Gallenkamp capillary apparatus and are uncorrected. Infrared spectra were recorded using KBr discs on a Perkin–Elmer Paragon 500 FT-IR spectrometer. ¹H NMR spectra were recorded on a Bruker DPX-200 spectrometer,

with chemical shifts δ reported in ppm unities relative to the internal standard TMS, using DMSO-*d*₆ as solvent. Mass spectra were obtained by using the Finnigan mass spectrometers, model MAT 8200 for low-resolution mass spectrometry (MS) and the MAT 95 for high resolution mass spectrometry (HRMS). Values for HRMS lie within the permitted limit intervals with resolution of 10000. The reactions were monitored by thin-layer chromatography (TLC) performed on silica gel plates prepared with Silica Gel 60 (PF-245 with gypsum, Merck) of a thickness of 0.25 mm. The developed chromatograms were visualized under ultraviolet light at 254–265 nm. For column chromatography, Merck Silica Gel 60 (230–400 mesh) was used. All common laboratory chemicals were purchased from commercial sources and used without further purification. Compounds **1a–h** and **2a–h** were prepared according to literature procedures.²²

6.2. General procedure for preparation of compounds **3a–h** and **4a–h**

To a stirred suspension of 0.01 mol of appropriate hydrazide in 5 mL of ethanol were added 3–4 drops of concentrated sulfuric acid, when the suspension changes into a clear solution. Then, the respective aromatic aldehyde (0.015 mol) previously dissolved in 5 mL of ethanol was added to the mixture at room temperature. After few seconds, a colored solid fell down and the mixture was stirred for 10 min prior to addition of 10 mL of water. After vacuum filtration, washing with cold water/ethanol 1:1 and then with cold water gave the desired compounds. Recrystallization from dioxane/water (1:1, v/v) mixture afforded the powdered final products. The yields, melting points, spectroscopic and spectrometric data are listed below for each compound.

6.3. 3-Phenyl-*N'*-[(4-acetamidophenyl)methylene]-1,2,4-oxadiazole-5-carbohydrazide (**3a**)

Mp 273–5 °C (from dioxane/H₂O); IR (KBr, cm⁻¹): ν = 3413 (N–H, acetamido), 3326 (N–H, acyl-hydrazone), 3037 (C–H, imine), 1708 (C=O, acetamido), 1671 (C=O, acyl-hydrazone), 1607 (N=C, imine), 1533 (N=C, heterocyclic); ¹H NMR (200 MHz, DMSO-*d*₆) δ : 12.7 (s, 1H, CONH), 10.2 (s, 1H, NHCOCH₃), 8.55 (s, 1H, N=CH), 8.10 (dd, J = ~4.0 Hz, 2H, *ortho*-oxadiazole ArH), 7.69 (s, 4H, ArH), 7.64–7.61 (m, 3H, *meta/para*-oxadiazole ArH), 2.07 (s, 3H, NHCOCH₃). MS (m/z , %): 349 (M⁺, 100), 204 (8), 147 (39), 118 (92), 103 (36), 43 (34), HRMS, Calcd (Found) for C₁₈H₁₅N₅O₃: 349.1174 (349.1171).

6.4. 3-(4-Methylphenyl)-*N'*-[(4-acetamidophenyl)methylene]-1,2,4-oxadiazole-5-carbohydrazide (**3b**)

Mp 286–8 °C (from dioxane/H₂O); IR (KBr, cm⁻¹): ν = 3420 (N–H, acetamido), 3317 (N–H, acyl-hydrazone), 3029 (C–H, imine), 1706 (C=O, acetamido), 1670 (C=O, acyl-hydrazone), 1609 (N=C, imine), 1532 (N=C, heterocyclic). ¹H NMR (200 MHz, DMSO-*d*₆) δ : 12.7 (s, 1H, CONH), 10.1 (s, 1H, NHCOCH₃), 8.55 (s, 1H, N=CH), 7.99 (d, J = 7.9 Hz, 2H, *ortho*-oxadiazole ArH), 7.69 (s, 4H, ArH), 7.42 (d, J = 7.8 Hz, 2H, *meta*-oxadiazole ArH), 2.40 (s, 3H, CH₃), 2.07 (s, 3H, NHCOCH₃). MS (m/z , %): 363 (M⁺, 72), 203 (25), 147 (44), 118 (100), 103 (30), 43 (48); HRMS, Calcd (Found) for C₁₉H₁₇N₅O₃: 363.1331 (363.1328).

6.5. 3-(4-Fluorophenyl)-*N'*-[(4-acetamidophenyl)methylene]-1,2,4-oxadiazole-5-carbohydrazide (**3c**)

Mp 287–9 °C (from dioxane/H₂O); IR (KBr, cm⁻¹): ν = 3424 (N–H, acetamido), 3341 (N–H, acyl-hydrazone), 3029 (C–H, imine), 1710 (C=O, acetamido), 1672 (C=O, acyl-hydrazone), 1608 (N=C,

imine), 1540 (N=C, heterocyclic). ^1H NMR (200MHz, DMSO- d_6) δ : 12.7 (s, 1H, CONH), 10.2 (s, 1H, NHC(=O)CH₃), 8.54 (s, 1H, N=CH), 8.15 (t, $J = 7.0$ Hz, 2H, *ortho*-oxadiazole ArH), 7.69 (s, 4H, ArH), 7.47 (t, $J = \sim 8.7$ Hz, 2H, *meta*-oxadiazole ArH), 2.06 (s, 3H, NHC(=O)CH₃). MS (m/z , %): 367 (M^+ , 100), 204 (5), 147 (26), 118 (52), 105 (23), 43 (19); HRMS, Calcd (Found) for C₁₈H₁₄N₅O₃F: 367.1080 (367.1083).

6.6. 3-(4-Chlorophenyl)-*N*-[(4-acetamidophenyl)methylene]-1,2,4-oxadiazole-5-carbohydrazide (3d)

Mp 292–4 °C (from dioxane/H₂O); IR (KBr, cm⁻¹) $\nu = 3440$ (N–H, acetamido), 3346 (N–H, acyl-hydrazone), 3033 (C–H, imine), 1703 (C=O, acetamido), 1670 (C=O, acyl-hydrazone), 1608 (N=C, imine), 1534 (N=C, heterocyclic). ^1H NMR (200 MHz, DMSO- d_6) δ : 12.8 (s, 1H, CONH), 10.2 (s, 1H, NHC(=O)CH₃), 8.54 (s, 1H, N=CH), 8.10 (d, $J = 8.5$ Hz, 2H, *ortho*-oxadiazole ArH), 7.70 (d, $J = 6.7$ Hz, 2H, *meta*-oxadiazole ArH), 7.69 (s, 4H, ArH), 2.06 (s, 3H, NHC(=O)CH₃). MS (m/z , %): 383/385 (M^+ , 100/34), 203 (7), 147 (31), 118 (69), 105 (28), 43 (22); HRMS, Calcd (Found) for C₁₈H₁₄N₅O₃Cl: 383.0785 (383.0791).

6.7. 3-(4-Bromophenyl)-*N*-[(4-acetamidophenyl)methylene]-1,2,4-oxadiazole-5-carbohydrazide (3e)

Mp >300 °C (from dioxane/H₂O); IR (KBr, cm⁻¹) $\nu = 3445$ (N–H, acetamido), 3341 (N–H, acyl-hydrazone), 3030 (C–H, imine), 1708 (C=O, acetamido), 1670 (C=O, acyl-hydrazone), 1608 (N=C, imine), 1539 (N=C, heterocyclic). ^1H NMR (200 MHz, DMSO- d_6) δ : 12.7 (s, 1H, CONH), 10.2 (s, 1H, NHC(=O)CH₃), 8.54 (s, 1H, N=CH), 8.02 (d, $J = 8.5$ Hz, 2H, *ortho*-oxadiazole ArH), 7.68 (d, $J = 8.5$ Hz, 2H, *meta*-oxadiazole ArH), 7.69 (s, 4H, ArH), 2.06 (s, 3H, NHC(=O)CH₃). MS (m/z , %): 427/429 (M^+ , 93/92), 203 (13), 147 (45), 118 (100), 105 (40), 43 (34); HRMS, Calcd (Found) for C₁₈H₁₄N₅O₃Br: 427.0280 (427.0279).

6.8. 3-(4-Nitrophenyl)-*N*-[(4-acetamidophenyl)methylene]-1,2,4-oxadiazole-5-carbohydrazide (3f)

Mp >300 °C (from dioxane/H₂O); IR (KBr, cm⁻¹) $\nu = 3420$ (N–H, acetamido), 3350 (N–H, acyl-hydrazone), 3045 (C–H, imine), 1708 (C=O, acetamido), 1667 (C=O, acyl-hydrazone), 1606 (N=C, imine), 1525 (N=C, heterocyclic); ^1H NMR (200 MHz, DMSO- d_6) δ : 12.8 (s, 1H, CONH), 10.2 (s, 1H, NHC(=O)CH₃), 8.55 (s, 1H, N=CH), 8.47 (d, $J = 9.0$ Hz, 2H, *ortho*-oxadiazole ArH), 8.35 (d, $J = 9.0$ Hz, 2H, *meta*-oxadiazole ArH), 7.69 (s, 4H, ArH), 2.06 (s, 3H, NHC(=O)CH₃). MS (m/z , %): 394 (M^+ , 100), 204 (12), 147 (23), 118 (77), 105 (32), 43 (38); HRMS, Calcd (Found) for C₁₈H₁₄N₆O₅: 394.1025 (394.1032).

6.9. 3-(4-Methoxyphenyl)-*N*-[(4-acetamidophenyl)methylene]-1,2,4-oxadiazole-5-carbohydrazide (3g)

Mp 294–6 °C (from dioxane/H₂O); IR (KBr, cm⁻¹) $\nu = 3424$ (N–H, acetamido), 3341 (N–H, acyl-hydrazone), 3044 (C–H, imine), 1703 (C=O, acetamido), 1667 (C=O, acyl-hydrazone), 1610 (N=C, imine), 1538 (N=C, heterocyclic). ^1H NMR (200 MHz, DMSO- d_6) δ : 12.7 (s, 1H, CONH), 10.2 (s, 1H, NHC(=O)CH₃), 8.54 (s, 1H, N=CH), 8.03 (d, $J = 8.9$ Hz, 2H, *ortho*-oxadiazole ArH), 7.69 (s, 4H, ArH), 7.16 (d, $J = 9.0$ Hz, 2H, *meta*-oxadiazole ArH), 3.85 (s, 3H, OCH₃), 2.07 (s, 3H, NHC(=O)CH₃). MS (m/z , %): 379 (M^+ , 100), 204 (9), 147 (35), 118 (36), 105 (20), 43 (16); HRMS, Calcd (Found) for C₁₉H₁₇N₅O₄: 379.1280 (379.1286).

6.10. 3-(4-Hydroxyphenyl)-*N*-[(4-acetamidophenyl)methylene]-1,2,4-oxadiazole-5-carbohydrazide (3h)

Mp 279–281 °C (from dioxane/H₂O); IR (KBr, cm⁻¹) $\nu = 3550$ –3200 (O–H), 3430 (N–H, acetamido), 3337 (N–H, acyl-hydrazone), 1706 (C=O, acetamido), 1667 (C=O, acyl-hydrazone), 1610 (N=C, imine), 1528 (N=C, heterocyclic). ^1H NMR (200 MHz, DMSO- d_6) δ : 12.7 (s, 1H, CONH), 10.3 (s, 1H, OH), 10.2 (s, 1H, NHC(=O)CH₃), 8.55 (s, 1H, N=CH), 7.94 (d, $J = 8.8$ Hz, 2H, *ortho*-oxadiazole ArH), 7.70 (s, 4H, ArH), 6.97 (d, $J = 8.8$ Hz, 2H, *meta*-oxadiazole ArH), 2.08 (s, 3H, NHC(=O)CH₃). MS (m/z , %): 365 (M^+ , 100), 204 (7), 147 (29), 118 (45), 105 (23), 43 (19); HRMS, Calcd (Found) for C₁₈H₁₅N₅O₄: 365.1124 (365.1123).

6.11. 3-Phenyl-*N*-[(4-hydroxyphenyl)methylene]-1,2,4-oxadiazole-5-carbohydrazide (4a)

98%; mp 240–1 °C (from dioxane/H₂O); IR (KBr, cm⁻¹): $\nu = 3486$ (O–H, br), 3248 (N–H), 3035 (C–H, imine), 1682 (C=O), 1607 (N=C, imine), 1587 (N=C, heterocyclic). ^1H NMR (200 MHz, DMSO- d_6) δ : 12.6 (s, 1H, NH), 10.1 (s, 1H, OH), 8.51 (s, 1H, N=CH), 8.09 (dd, $J = \sim 7.0$ Hz, 2H, *ortho*-oxadiazole ArH), 7.64–7.57 (m, 5H, ArH), 6.85 (d, $J = 8.5$ Hz, 2H, *ortho*-OH ArH). MS (m/z , %): 308 (M^+ , 53), 189 (22), 145 (15), 119 (100), 106 (58), 77 (41); HRMS, Calcd (Found) for C₁₆H₁₂N₄O₃: 308.0909 (308.0913).

6.12. 3-(4-Methylphenyl)-*N*-[(4-hydroxyphenyl)methylene]-1,2,4-oxadiazole-5-carbohydrazide (4b)

Mp 235–7 °C (from dioxane/H₂O); IR (KBr, cm⁻¹): $\nu = 3441$ (O–H, br), 3320 (N–H), 3030 (C–H, imine), 1673 (C=O), 1604 (N=C, imine), 1547 (N=C, heterocyclic); ^1H NMR (200 MHz, DMSO- d_6) δ : 12.6 (s, 1H, NH), 10.1 (s, 1H, OH), 8.50 (s, 1H, N=CH), 7.98 (d, $J = 8.2$ Hz, 2H, *ortho*-oxadiazole ArH), 7.59 (d, $J = 8.5$ Hz, 2H, *meta*-OH ArH), 7.42 (d, $J = 8.2$ Hz, 2H, *meta*-oxadiazole ArH), 6.85 (d, $J = 8.7$ Hz, 2H, *ortho*-OH ArH), 2.40 (s, 3H, CH₃). MS (m/z , %): 322 (M^+ , 92), 203 (100), 159 (18), 119 (64), 106 (59), 77 (20); HRMS, Calcd (Found) for C₁₇H₁₄N₄O₃: 322.1065 (322.1063).

6.13. 3-(4-Fluorophenyl)-*N*-[(4-hydroxyphenyl)methylene]-1,2,4-oxadiazole-5-carbohydrazide (4c)

Mp 260–2 °C (from dioxane/H₂O); IR (KBr, cm⁻¹): $\nu = 3362$ (O–H, br), 3310 (N–H), 3030 (C–H, imine), 1690 (C=O), 1608 (N=C, imine), 1562 (N=C, heterocyclic); ^1H NMR (200 MHz, DMSO- d_6) δ : 12.6 (s, 1H, NH), 10.1 (s, 1H, OH), 8.50 (s, 1H, N=CH), 8.14 (dd, $J = \sim 8.8$ Hz, 2H, *ortho*-oxadiazole ArH), 7.59 (d, $J = 8.7$ Hz, 2H, *meta*-OH ArH), 7.47 (t, $J = 8.8$ Hz, 2H, *meta*-oxadiazole ArH), 6.85 (d, $J = 8.5$ Hz, 2H, *ortho*-OH ArH). MS (m/z , %): 326 (M^+ , 100), 207 (39), 163 (18), 119 (79), 106 (41), 77 (11); HRMS, Calcd (Found) for C₁₆H₁₁N₄O₃F: 326.0815 (326.0804).

6.14. 3-(4-Chlorophenyl)-*N*-[(4-hydroxyphenyl)methylene]-1,2,4-oxadiazole-5-carbohydrazide (4d)

Mp 272–4 °C (from dioxane/H₂O); IR (KBr, cm⁻¹): $\nu = 3442$ (O–H, br), 3307 (N–H), 3029 (C–H, imine), 1698 (C=O), 1604 (N=C, imine), 1583 (N=C, heterocyclic); ^1H NMR (200 MHz, DMSO- d_6) δ : 12.6 (s, 1H, NH), 10.1 (s, 1H, OH), 8.50 (s, 1H, N=CH), 8.10 (d, $J = 8.7$ Hz, 2H, *ortho*-oxadiazole ArH), 7.70 (d, $J = 8.7$ Hz, 2H, *meta*-OH ArH), 7.59 (d, $J = 8.7$ Hz, 2H, *meta*-oxadiazole ArH), 6.85 (d, $J = 8.5$ Hz, 2H, *ortho*-OH ArH). MS (m/z , %): 342/344 (M^+ , 37/15), 223/225 (43/13), 179 (8), 119 (100), 106 (68), 77 (21); HRMS, Calcd (Found) for C₁₆H₁₁N₄O₃Cl: 342.0519 (342.0511).

6.15. 3-(4-Bromophenyl)-N'-[(4-hydroxyphenyl)methylene]-1,2,4-oxadiazole-5-carbohydrazide (4e)

Mp 278–280 °C (from dioxane/H₂O); IR (KBr, cm⁻¹): ν = 3447 (O–H, br), 3307 (N–H), 3028 (C–H, imine), 1698 (C=O), 1605 (N=C, imine), 1582 (N=C, heterocyclic); ¹H NMR (200 MHz, DMSO-*d*₆) δ : 12.6 (s, 1H, NH), 10.1 (s, 1H, OH), 8.50 (s, 1H, N=CH), 8.02 (d, *J* = 8.7 Hz, 2H, *ortho*-oxadiazole ArH), 7.84 (d, *J* = 8.7 Hz, 2H, *meta*-OH ArH), 7.59 (d, *J* = 8.7 Hz, 2H, *meta*-oxadiazole ArH), 6.85 (d, *J* = 8.5 Hz, 2H, *ortho*-OH ArH). MS (*m/z*, %): 386/388 (M⁺, 52/52), 267/269 (44/44), 223/225 (6/7), 119 (100), 106 (51), 77 (14); HRMS, Calcd (Found) for C₁₆H₁₁N₄O₃Br: 386.0014 (386.0005).

6.16. 3-(4-Nitrophenyl)-N'-[(4-hydroxyphenyl)methylene]-1,2,4-oxadiazole-5-carbohydrazide (4f)

Mp > 300 °C (from dioxane/H₂O); IR (KBr, cm⁻¹): ν = 3452 (O–H, br), 3364 (N–H), 3069 (C–H, imine), 1695 (C=O), 1606 (N=C, imine), 1587 (N=C, heterocyclic). ¹H NMR (200 MHz, DMSO-*d*₆) δ : 12.7 (s, 1H, NH), 10.1 (s, 1H, OH), 8.50 (s, 1H, N=CH), 8.46 (d, *J* = 9.0 Hz, 2H, *ortho*-oxadiazole ArH), 8.34 (d, *J* = 9.2 Hz, 2H, *meta*-oxadiazole ArH), 7.59 (d, *J* = 8.7 Hz, 2H, *meta*-OH ArH), 6.85 (d, *J* = 8.5 Hz, 2H, *ortho*-OH ArH). MS (*m/z*, %): 353 (M⁺, 74), 234 (2), 190 (4), 119 (100), 106 (36), 77 (7); HRMS, Calcd (Found) for C₁₆H₁₁N₅O₅: 353.0760 (353.0767).

6.17. 3-(4-Methoxyphenyl)-N'-[(4-hydroxyphenyl)methylene]-1,2,4-oxadiazole-5-carbohydrazide (4g)

Mp 219–221 °C (from dioxane/H₂O); IR (KBr, cm⁻¹): ν = 3444 (O–H, br), 3340 (N–H), 3010 (C–H, imine), 1681 (C=O), 1604 (N=C, imine), 1551 (N=C, heterocyclic). ¹H NMR (200 MHz, DMSO-*d*₆) δ : 12.6 (s, 1H, NH), 10.1 (s, 1H, OH), 8.50 (s, 1H, N=CH), 8.03 (d, *J* = 8.9 Hz, 2H, *ortho*-oxadiazole ArH), 7.59 (d, *J* = 8.7 Hz, 2H, *meta*-OH ArH), 7.15 (d, *J* = 8.9 Hz, 2H, *meta*-oxadiazole ArH), 6.82 (d, *J* = 8.5 Hz, 2H, *ortho*-OH ArH), 3.85 (s, 3H, OCH₃). MS (*m/z*, %): 338 (M⁺, 93), 219 (99), 175 (14), 148 (100), 133 (65), 119 (50), 106 (53), 77 (21); HRMS, Calcd (Found) for C₁₇H₁₄N₄O₄: 338.1015 (338.1008).

6.18. 3-(4-Hydroxyphenyl)-N'-[(4-hydroxyphenyl)methylene]-1,2,4-oxadiazole-5-carbohydrazide (4h)

Mp 263–5 °C (from dioxane/H₂O); IR (KBr, cm⁻¹): ν = 3459 (O–H, br), 3319 (N–H), 3020 (C–H, imine), 1677 (C=O), 1598 (N=C, imine), 1556 (N=C, heterocyclic). ¹H NMR (200 MHz, DMSO-*d*₆) δ : 12.6 (s, 1H, NH), 10.3 (s, 1H, *para*-oxadiazole OH), 10.1 (s, 1H, OH), 8.49 (s, 1H, N=CH), 7.92 (d, *J* = 8.7 Hz, 2H, *ortho*-oxadiazole ArH), 7.59 (d, *J* = 8.7 Hz, 2H, *meta*-OH ArH), 6.95 (d, *J* = 8.8 Hz, 2H, *meta*-oxadiazole ArH), 6.85 (d, *J* = 8.7 Hz, 2H, *ortho*-OH ArH). MS (*m/z*, %): 324 (M⁺, 35), 205 (45), 161 (10), 134 (38), 119 (55), 106 (37), 77 (11), 28 (100); HRMS, Calcd (Found) for C₁₆H₁₂N₄O₄: 324.0858 (324.0859).

6.19. In vitro cytotoxicity

The cytotoxicity of the compounds was determined using BALB/c mice splenocytes (5 × 10⁶ cells well⁻¹) cultured in 96-well plates in Dulbecco's Modified Eagle's Medium (DMEM, Sigma Chemical Co., St. Louis, MO) supplemented with 10% of fetal calf serum (FCS; Cultilab, Campinas, SP, Brazil) and 50 μg mL⁻¹ of gentamycin (Novafarma, Anápolis, GO, Brazil). Each compound was evaluated in three concentrations (1.1, 3.3, 11, 33, 100 μg mL⁻¹), in triplicate. Cultures were incubated in the presence of ³H-thymidine (1 μCi well⁻¹) for 24 h at 37 °C and 5% CO₂. After this period, the content of the plate was harvested to determine the ³H-thymidine incorpo-

ration using a beta-radiation counter (Multilabel Reader, Hidex, Turku, Finland). The cytotoxicity of the compounds was determined by comparing the percentage of ³H-thymidine incorporation (as indicator of viability cell) of drug-treated wells in relation to untreated wells. Non-cytotoxic concentrations were defined as those causing a reduction of ³H-thymidine incorporation below 10% in relation to untreated controls.

6.20. In vitro antiproliferative activity

Epimastigotes of *T. cruzi* (Y strain)³⁴ were cultivated at 26 °C in liver infusion tryptose medium (LIT) supplemented with 10% fetal calf serum, 1% hemin, 1% R9 medium and 50 μg mL⁻¹ gentamycin. Parasites (10⁶ cells mL⁻¹) were cultured in a fresh medium in the absence or in the presence of the compounds being tested (from stock solution in DMSO). Cell growth was determined after 11 days of culture by counting viable forms in a hemacytometer, in triplicate. The compounds were used from a stock solution in DMSO. To determine the IC₅₀, cultures of Y strain epimastigotes in the presence of different concentrations (0.1, 1.0, 5, 10, 25, 50, 100 μg mL⁻¹) of the compounds were evaluated after 11 days as described above. IC₅₀ calculation was carried out using non-linear regression on Prism 4.0 GraphPad software. Y strain *T. cruzi* trypomastigotes were obtained from culture supernatants of Vero cell line at 37 °C and placed in 96-well plates (4 × 10⁵ well⁻¹) in DMEM medium supplemented with 10% FCS and 50 μg mL⁻¹ gentamycin. Viable parasites were counted in a hemacytometer 24 h after addition of compounds by way of trypan blue exclusion. The percentage of inhibition was calculated in relation to untreated cultures. The same procedures were performed for **Bdz** (reference drug) and **GV** (reference for trypomastigote assay) and vehicle alone, DMSO as blank.

6.21. Toxicological tests in mice

The selected compounds were resuspended in 100 μL [30% DMSO:70% H₂O, v/v] per dose of 100 mg/kg weight, using 6 animals per group. The treated animals were monitored for signs of general toxicity, during 72 h after the treatment. The survival of drug-treated mice was evaluated and compared to untreated animals, which received only 100 μL of solution [30% DMSO:70% H₂O, v/v]. This experimental protocol was approved and supervised by the Ethics Committee of HEMOPE Hospital (Recife, PE, Brazil).

Acknowledgements

This work was supported by grants from the CNPq (# 479982/2008-2), FACEPE (#APQ-0123-4.03/08), RENORBIO and INCT-CNPq. D.R.M.M and M.B.P.S are supported by CNPq. We acknowledge the Laboratory of Medicinal Theoretical Chemistry (UFPE) by the access of software and HEMOPE Hospital for supplying mice for toxicological tests. Authors are also thankful to Mr. Thomas Dulks and Mrs. Dorit Kamken (University of Bremen, Germany) for recording the MS and HRMS of all compounds and José F. O. Costa (FIOCRUZ) for his technical assistance in the cytotoxicity assay.

References and notes

- Barrett, M. P.; Burchmore, R. J. S.; Stich, A.; Lazzari, J. O.; Frasca, A. C.; Cazzulo, J. J.; Krishna, S. *Lancet* **2003**, 362, 1469.
- Coura, J. R. *Mem. Inst. Oswaldo Cruz* **2007**, 102, 113.
- (a) Urbina, J. A.; Docampo, R. *Trends Parasitol.* **2003**, 19, 495; (b) Cerecetto, H.; Gonzalez, M. *Mini-Rev. Med. Chem.* **2008**, 8, 1355; (c) Azevedo, W. F., Jr.; Soares, M. B. P. *Curr. Drug Targets* **2009**, 11, 193; (d) Hunter, W. N. J. *Biol. Chem.* **2009**, 284, 11749; (e) Brenk, R.; Schipani, A.; James, D.; Krasowski, A.; Gilbert, I. H.; Frearson, J.; Wyatt, P. G. *ChemMedChem* **2008**, 3, 435.
- Caffrey, C. R.; Scory, S.; Steverding, D. *Curr. Drug Targets* **2000**, 1, 155.

5. Siegel, R. L. K.; Comini, M. A. *Biochim. Biophys. Acta* **2008**, *1780*, 1236.
6. Neres, J.; Bryce, R. A.; Douglas, K. T. *Drug Discovery Today* **2008**, *13*, 110.
7. Moreira, D. R. M.; Leite, A. C. L.; Santos, R. R.; Soares, M. B. P. *Curr. Drug Targets* **2009**, *10*, 212.
8. Cazullo, J. J. *Curr. Top. Med. Chem.* **2002**, *2*, 1257.
9. (a) Scharfstein, J.; Schmitz, V.; Morandi, V.; Capella, M. M.; Lima, A. P.; Morrot, A.; Juliano, L.; Müller-Esterl, W. *J. Exp. Med.* **2000**, *192*, 1289; (b) Aparicio, I. M.; Scharfstein, J.; Lima, A. P. C. A. *Infect. Immun.* **2004**, *72*, 5892.
10. Steverding, D.; Caffrey, C. R.; Sajid, M. *Mini-Rev. Med. Chem.* **2006**, *6*, 1025.
11. (a) Roush, W. R.; González, F. V.; McKerrow, J. H.; Hansell, E. *Bioorg. Med. Chem. Lett.* **1998**, *8*, 2809; (b) Roush, W. R.; Cheng, J.; Reed, B. K.; Alvarez-Hernandez, A.; Hansell, E.; McKerrow, J. H.; Engel, C. J. *Bioorg. Med. Chem. Lett.* **2001**, *11*, 2759; (c) Jaishankar, P.; Doyle, P. S.; Hansell, E.; McKerrow, J. H.; Zhao, D. M.; Renslo, A. R. *Bioorg. Med. Chem. Lett.* **2008**, *18*, 624.
12. Li, R.; Chen, X.; Gong, B.; Selzer, P. M.; Li, S.; Davidson, E.; Kurzban, G.; Miller, R. E.; Nuzum, E.; McKerrow, J. H.; Fletterick, R. J.; Gilmore, S. A.; Craik, C. S.; Kuntz, I. D.; Cohen, F. E.; Kenyon, G. L. *Bioorg. Med. Chem.* **1996**, *4*, 1421.
13. (a) Troeberg, L.; Chen, X.; Cheng, M.; Kenyon, G. L.; Flaherty, T. M.; Hua, H.; Cohen, F. E.; Springer, C.; Lonsdale-Eccles, J. D.; Morty, R. E.; McKerrow, J. H.; Coetzer, T. H. T. *Mol. Med.* **2000**, *6*, 660; (b) Selzer, P. M.; Pingel, S.; Hsieh, I.; Ugele, B.; Chan, V. J.; Engel, J. C.; Bogyo, M.; Russel, D. G.; Sakanari, J. A.; McKerrow, J. H. *Proc. Natl. Acad. Sci. U.S.A.* **1999**, *96*, 11015; (c) Caffrey, C. R.; Schanz, M.; Nkemgu-Njinkeng, J.; Brush, M.; Hansell, E.; Cohen, F. E.; Flaherty, T. M.; McKerrow, J. H.; Steverding, D. *Int. J. Antimicrob. Agents* **2002**, *19*, 227; (d) Melnyk, P.; Leroux, V.; Sergheraert, C.; Grellier, P. *Bioorg. Med. Chem. Lett.* **2006**, *16*, 31.
14. Ifa, D. R.; Rangel, C. R.; Alencastro, R. B.; Fraga, C. A. M.; Barreiro, E. J. *J. Mol. Struct.* **2000**, *505*, 11.
15. Rodrigues, C. R.; Flaherty, T. F.; McKerrow, J. H.; Springer, C.; Cohen, F. E. *Bioorg. Med. Chem. Lett.* **2002**, *12*, 1537.
16. Romeiro, N. C.; Aguirre, G.; Hernández, P.; González, M.; Cerecetto, H.; Aldana, I.; Pérez-Silanes, S.; Monge, A.; Barreiro, E. J.; Lima, L. M. *Bioorg. Med. Chem.* **2009**, *17*, 641.
17. (a) Vera-Divaio, M. A. F.; Freitas, A. C.; Castro, H. C.; Albuquerque, S.; Cabral, L. M.; Rodrigues, C. R.; Albuquerque, M. G.; Martins, R. C. A.; Henriques, M. G. O.; Dias, L. R. S. *Bioorg. Med. Chem.* **2009**, *17*, 295; (b) Zanatta, N.; Amaral, S. S.; Santos, J. M.; de Mello, D. L.; Fernandes, L. D. S.; Bonacorso, H. G.; Martins, M. A. P.; Andricopulo, A. D.; Borchhardt, D. M. *Bioorg. Med. Chem.* **2008**, *16*, 10236.
18. (a) Fraga, C. A. M.; Barreiro, E. J. *Curr. Med. Chem.* **2006**, *13*, 167; (b) Rollas, S.; Küçükgül, S. G. *Molecules* **2007**, *12*, 1910.
19. For an excellent definition of privileged structures, see: Duarte, C. D.; Barreiro, E. J.; Fraga, C. A. M. *Mini-Rev. Med. Chem.* **2007**, *7*, 1108.
20. (a) Cerecetto, H.; Maio, R. D.; González, M.; Risso, M.; Saenz, P.; Seoane, G.; Denicola, A.; Peluffo, G.; Quijano, C.; Olea-Azar, C. *J. Med. Chem.* **1999**, *42*, 1945; (b) Havens, C.; Bryant, N.; Asher, L.; Lamoreaux, L.; Perfetto, S.; Brendle, J.; Werbovetz, K. *Mol. Biochem. Parasitol.* **2000**, *110*, 223; (c) Cottrell, D. M.; Capers, J.; Salem, M. M.; DeLuca-Fradley, K.; Croft, S. L.; Werbovetz, K. A. *Bioorg. Med. Chem.* **2004**, *13*, 2815; (d) Sayed, A. A.; Simeonov, A.; Thomas, C. J.; Inglese, J.; Austin, C. P.; Williams, D. L. *Nat. Med.* **2008**, *14*, 407.
21. (a) Jakopin, Z.; Dolenc, M. S. *Curr. Org. Chem.* **2008**, *12*, 850; (b) Borg, S.; Estenne-Bouthou, G.; Luthman, K.; Csoregh, I.; Hesselink, W.; Hacksell, U. *J. Org. Chem.* **1995**, *60*, 3112; (c) Boeglin, D.; Cantel, S.; Heitz, A.; Martinez, J.; Fehrentz, J. A. *Org. Lett.* **2003**, *5*, 4465.
22. Leite, L. F. C. C.; Ramos, M. N.; da Silva, J. B. P.; Miranda, A. L. P.; Fraga, C. A. M.; Barreiro, E. J. *Farmacol.* **1999**, *54*, 747.
23. Santos-Filho, J. M.; de Lima, J. G.; Leite, L. F. C. C.; Ximenes, E. A.; da Silva, J. B. P.; Lima, P. C.; Pitta, I. R. *Heterocycl. Commun.* **2005**, *11*, 29.
24. (a) Bezerra-Netto, H. J. C.; Lacerda, D. I.; Miranda, A. L. P.; Alves, H. M.; Barreiro, E. J.; Fraga, C. A. M. *Bioorg. Med. Chem.* **2006**, *14*, 7924; (b) Carvalho, S. A.; Lopes, F. A. S.; Wardell, S. M. S. V.; Salomão, K.; Castro, S. L.; Romeiro, N. C.; Silva, E. F.; Fraga, C. A. M. *Bioorg. Med. Chem.* **2008**, *16*, 413.
25. Dewar, M. J. S.; Zois, E. G.; Healy, E. F.; Stewart, J. J. P. *J. Am. Chem. Soc.* **1985**, *107*, 3902.
<http://www.CACheSoftware.com>.
27. Choe, Y.; Brinen, L. S.; Price, M. S.; Engel, J. C.; Lange, M.; Grisostomi, C.; Weston, S. C.; Pallai, P. V.; Cheng, H.; Hardy, L. W.; Hartsough, D. S.; McMakin, M.; Tilton, R. F.; Baldino, C. M.; Craik, C. S. *Bioorg. Med. Chem.* **2005**, *13*, 2141.
28. <http://www.rcsb.org/pdb>.
29. http://www.ccdc.cam.ac.uk/products/gold_suite/.
30. Nogueira, R. C.; Oliveira-Costa, J. F.; de Sá, M. S.; dos Santos, R. R.; Soares, M. B. P. *Curr. Drug Targets* **2009**, *10*, 291.
31. DeLano, W. L. The PYMOL Molecular Graphics System, DeLano Scientific, San Carlos, CA, USA, 2002, in <http://www.pymol.org>.
32. Memic, A.; Spaller, M. R. *ChemBioChem* **2008**, *9*, 2793.
33. ALOPS 2.1 Database was Used Accessing the Virtual Computational Chemistry Laboratory (VCCLABS); <http://www.vcclab.org>.
34. Leite, A. C. L.; Moreira, D. R. M.; Cardoso, M. V. O.; Hernandez, M. Z.; Pereira, V. R. A.; Silva, R. O.; Kiperstok, A. C.; Lima, M. S.; Soares, M. B. P. *ChemMedChem* **2007**, *2*, 1339.